

# Aortic valve cusp vessel density: Relationship with tissue thickness

K. L. Weind, PhD<sup>a,b</sup>  
 C. G. Ellis, PhD<sup>b</sup>  
 D. R. Boughner, MD, PhD<sup>a,b,c</sup>

**Objectives:** The presence of a microvasculature within aortic cusps implies that tissue oxygen requirements exceed the amount deliverable by diffusion from the tissue surfaces alone. For the design of a successful tissue-engineered valve replacement, the effect of diffusion distance (tissue thickness) on oxygen delivery must be considered. We therefore examined in normal aortic valve cusps the relationship between the presence of microvessels and the tissue thickness.

**Methods:** Thirty porcine aortic valve cusps were excised and examined after cusp microvessels were pressure filled with a carbon particle solution. Cusp images were captured for stereographic vessel density analysis, and cusp thickness was determined with a radiographic technique. Histologic cross-sections were evaluated to determine vessel depth from the cusp surface.

**Results:** Cusp basal regions measured 0.69 to 0.86 mm in thickness, significantly thicker ( $P = .001$ ) than the rest of the cusp, which measured 0.36 to 0.48 mm. In general a vascular bed was present when cusp thickness exceeded 0.5 mm, with a median value of 5.16 vessels/mm<sup>3</sup>.

**Conclusions:** From published values of arterial wall oxygen consumption and diffusivity, we predicted that the probable maximum oxygen diffusion distance for valve tissue would be about 0.2 mm. This was consistent with our physical findings, which implies that central tissue anoxia is avoided by the capillary bed. An avascular tissue-engineered valve metabolically similar to an aortic valve should therefore not exceed a thickness of approximately 0.40 mm.

From The Heart Valve Laboratory,<sup>a</sup> The John P. Robarts Research Institute, The Department of Medical Biophysics,<sup>b</sup> University of Western Ontario, and The Division of Cardiology,<sup>c</sup> London Health Sciences Centre, University Campus, London, Ontario, Canada.

Supported by a grant-in-aid T3573 from the Heart and Stroke Foundation of Ontario and the Medical Research Council of Canada. K.L.W. was supported in part by the Ontario Graduate Student for Science and Technology Scholarship Programme.

Received for publication March 9, 2001; revisions requested April 13, 2001; revisions received June 22, 2001; accepted for publication Aug 15, 2001.

Address for reprints: Derek R. Boughner, MD, PhD, London Health Sciences Centre, University Campus, 339 Windermere Rd, London, Ontario N6A 5A5, Canada (E-mail: derek.boughner@lhsc.on.ca).

J Thorac Cardiovasc Surg 2002;123:333-40

Copyright © 2002 by The American Association for Thoracic Surgery

0022-5223/2002 \$35.00 + 0 12/1/119696

doi:10.1067/mtc.2002.119696

The search for an ideal valve replacement device has recently been extended to the concept of a bioengineered “living” valve, constructed from a biodegradable skeleton with cellular implants.<sup>1,2</sup> Current glutaraldehyde-fixed bioprostheses remain vulnerable to premature tissue failure,<sup>3</sup> with their durability shown to be substantially less than that observed for mechanical devices.<sup>4</sup> Such glutaraldehyde-fixed implants are acellular, with the tissue containing no intrinsic repair mechanism. To avoid this problem and to provide replacement valves with living cells and therefore a means for tissue repair, cryopreserved bioprostheses have been recommended.<sup>5</sup> However, it appears that the tissue failure rate of cryopreserved valves is similar to that of glutaraldehyde-fixed implants.<sup>6</sup> Explanations for this finding are that either the cryopreservation process itself or the new environment of these valve cells hinders their viability, resulting in an essentially acellular implant also missing repair abilities.<sup>7</sup> Indeed, if these valves contained large numbers of cells, postimplantation rejection might also play a role in valve implant destruction.<sup>8,9</sup> For these reasons strong interest has developed in tissue-engineered alternatives containing living cells metabolically capable of maintaining valve structure. The recommendation is that such cells could be seeded from the recipi-

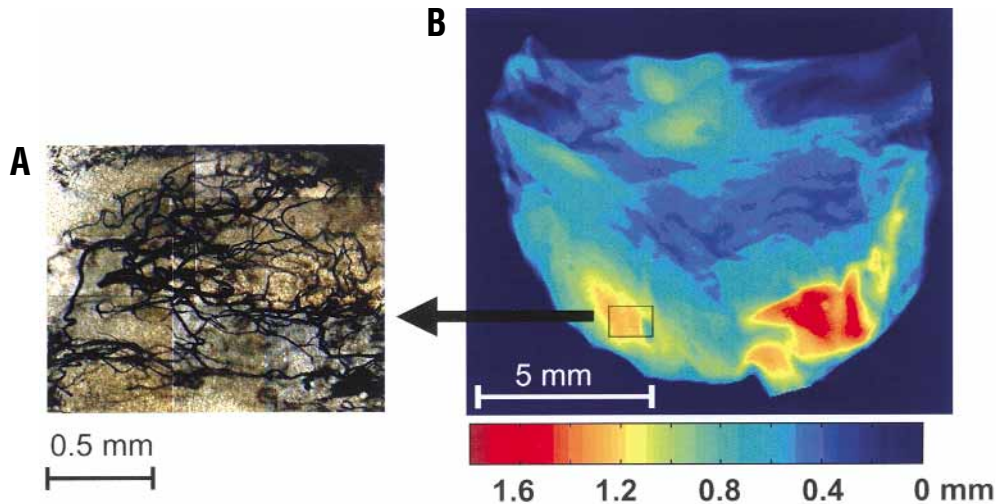


**Figure 1. A, Magnified region of interest in base of cusp (4× magnification) demonstrating microvasculature filled with Aquablack. B, Example of thickness map of whole cusp generated from radiographic thickness data.**

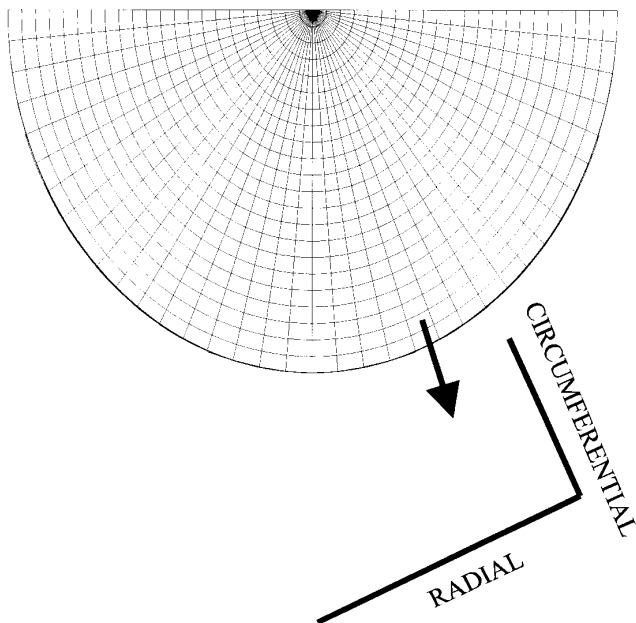


**Figure 2. Schematic of grid in circumferential and radial directions overlaid on full images of cusps for stereographic vessel density analysis.**

ent, thus bypassing any antigenic rejection issues.<sup>10,11</sup> Ultimately, for the design of a successful tissue-engineered replacement, a full understanding of how the native aortic valve sustains its metabolic functions is required.

In our earlier article the extent of the porcine aortic valve microcirculation was examined, and our analysis showed the vessel supply to lie predominantly in the basal region of

all three cusps.<sup>12</sup> Although it is generally believed that the aortic valve relies on oxygen diffusing from its surfaces to maintain its metabolic needs,<sup>13</sup> the presence of a vasculature in healthy valves suggested that this oxygenation pathway may not always be adequate.

We hypothesized that the intrinsic circulation of the aortic valve cusps may play a necessary role in oxygen delivery, much like the vasa vasorum of the aorta, but that vessels would exist only in areas where tissue thickness limits oxygen diffusion from the cusp surfaces. We therefore set out to measure and compare vessel density and tissue thickness to test this hypothesis and provide some useful parameters to be considered in the design of tissue-engineered valves.

## Materials and Methods

### Specimen Retrieval and Microvascular Filling

Ten whole pig hearts (30 cusps) were collected from a local abattoir after slaughter, and the coronary circulation was rinsed and pressure filled with Aquablack (Sun Chemical Canada, Brampton, Ontario, Canada), a suspended carbon particle solution, to allow vessel visualization according to a previously described protocol.<sup>12</sup> After this the cusps were fixed in 10% formaldehyde for storage purposes. Analysis was carried out on all three aortic valve cusps (left coronary, right coronary, and noncoronary) so that any differences between cusps could be discriminated.

### Cusp Microcirculation Analysis

To evaluate the density of vessels, each whole cusp was placed under a coverslip and viewed with an inverted microscope at 4 times magnification (numeric aperture 0.13) with a stabilized power supply to transilluminate the tissue at a constant light intensity. With a 24-bit red-green-blue charged-couple device camera (Japan Victor Corporation TK-1070U) connected to a Silicon

Graphics Indy image analysis work station (Silicon Graphics, Inc, Mountain View, Calif), cusp images (field of view  $2.1 \times 1.6$  mm) were captured frame by frame and averaged for better signal-to-noise ratio with software developed in our laboratory. Reconstruction of entire cusps was then performed on a personal computer with commercially available software (Adobe Photoshop; Adobe Systems Inc, San Jose, Calif). A section of the cusp showing microvasculature filled with Aquablack can be seen in Figure 1, A.

A schematic grid (Figure 2) was overlaid in the radial and circumferential directions for vessel density analysis. With Sigma Scan (SPSS Inc, Chicago, Ill) and stereographic counting principles,<sup>14</sup> the number of vessels per unit cusp area was determined by first counting the number of vessels crossing 2 sides of every 4-sided quadrant of the grid. Vessels crossing along the radial and circumferential sides of each quadrant were counted and recorded separately to analyze any preferred vessel orientation, because non-random orientation must be considered in stereographic analysis. Because the quadrants were rectangular and not square, the number of vessels per unit length was necessary for comparing the number of vessels aligned in the radial direction versus the circumferential direction. In addition, vessel diameters as well as the number of quadrants within the grid containing vessels were recorded. Because vessel counting was carried out by a single author (K.L.W.), random quadrants were recounted to determine intra-observer variability. On the basis of our previous results investigating the blood supply within the cusps,<sup>12</sup> cusps were divided into two main regions for all analyses; the base, found to contain most of the intrinsic circulation, and the rest of the cusp, found to be relatively avascular (Figure 3). After this, a Movats pentachrome-stained histologic cross-section of each of the samples was evaluated to determine the location of the microcirculation within the three layers of the cusp.

### Thickness Mapping

To determine the thickness of these cusps, we used a radiographic thickness imaging technique developed in our laboratory. This entailed taking a low-energy, high-resolution x-ray image of the valve cusps. Because the attenuation of the x-ray beam through the tissue depends on its thickness, the x-ray image could be converted into a thickness map by comparing the cusp x-ray attenuation values with those of a reference with a known thickness.

The imaging system contained a 200- $\mu$ m beryllium window fixed tungsten anode microfocuss source (Kevex X-Ray, Scotts Valley, Calif) and a digital x-ray detector consisting of a cesium iodide input phosphor coated onto a fiberoptic taper bound to a charged-coupled device detector (Hamamatsu Corporation, Bridgewater, NJ). It was developed to allow a thickness image of specimens as large as 32 by 24 mm in the x and y directions and optimized so that the thickness of discrete 50  $\times$  50-mm areas (pixels) across a sample could be separately analyzed.

Fixed tissue was patted dry before being mounted on a jig in front of the x-ray detector for image acquisition. Scotch Double-Stick Tape (3M Commercial Office Supply Division, St Paul, Minn) was used to help keep the specimen in place. Care was taken to ensure that the mounted tissue was lying flat with minimal stretching or deformation. Cusps were placed with the ven-

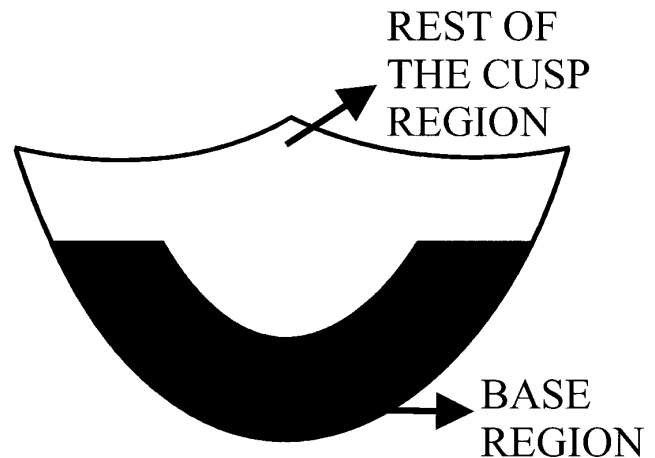


**Figure 3. Schematic of porcine aortic valve cusp outlining regions for analysis: base (black) and rest of cusp (white).**

tricularis (flatter side) down. A calibration step wedge milled from the tissue-mimicking substance MS15 (Gammex RMI, Middleton, Wis) was also mounted within the scanner's field of view so that each x-ray image of the cusp would also contain the calibration wedge. MS15 is an epoxy-based resin optimized with particulate fillers to have a linear attenuation coefficient at the energy range of this experiment to within a few percent of that of tissue.<sup>15,16</sup> Although there is no specific tissue mimic for heart valves, extensive analysis of various tissue mimics by White<sup>15</sup> has shown that MS15, a tissue substitute developed to mimic muscle, has a linear attenuation coefficient also within a few percent of water. Because the valve has been found to be composed of approximately 90% water<sup>17</sup> and tissues with a high percentage of water have similar attenuation coefficients, we considered this an ideal calibrator for our radiographic thickness measurements. This wedge was used as an "in-image" calibration to determine the thickness value for each 50  $\times$  50-mm pixel within the sample.

Digital radiographs of the samples and step wedge were acquired at a tube potential of 35 kV peak and 2 mAs. Bright-field (images with sample holder and double-sided tape but no tissue) and dark-field (images without x-ray source on) images were collected to correct for detector-to-detector variation and fixed pattern electronic noise, respectively. Finally, the images were corrected for geometric distortion in the fiberoptic taper stage of the detector through the use of a registration grid phantom.<sup>18</sup>

Our previous work has shown that fixation with 10% formaldehyde causes an increase in thickness presumably related to the cross-linking of collagen.<sup>19</sup> Scott<sup>17</sup> has also reported that the amount of collagen is variable within the cusp, and therefore fixation effects might also be inconsistent throughout the tissue. To examine fixation effects and determine a correction factor for the two regions of analysis within the cusps, 14 cusps were radiographically scanned fresh according to the preceding protocol, fixed in 10% formaldehyde for 1 week at 4°C to ensure complete fixation,<sup>17</sup> and then rescanned. Correction factors were obtained from comparisons between matched fresh and fixed thickness results.

**TABLE 1A. Vessels per millimeter along grid lines in the circumferential and radial directions**

Cusp	Radial		Circumferential		Combined	
	Base region	Rest of cusp	Base region	Rest of cusp	Base region	Rest of cusp
Left coronary	1.98 ± 1.91	0.04 ± 0.05	1.43 ± 1.63	0.11 ± 0.17	3.41 ± 3.51	0.15 ± 0.22
Noncoronary	2.17 ± 2.71	0.13 ± 0.19	1.96 ± 2.58	0.11 ± 0.18	4.12 ± 5.27	0.27 ± 0.36
Right coronary	2.25 ± 3.99	0.22 ± 0.46	2.17 ± 3.05	0.24 ± 0.49	4.42 ± 6.82	0.47 ± 0.94
Mean					3.98 ± 5.21	0.29 ± 0.59

Data are mean ± SD.

**TABLE 1B. Two-way repeated-measures ANOVA results comparing vessel density results in the circumferential versus radial directions and in the base region versus the rest of the cusp for all three cusps**

	<i>P</i> value
Circumferential versus radial	
Left coronary versus noncoronary versus right coronary cusp	.507
Circumferential vs radial	.285
Interaction	.809
Base versus rest of cusp	
Left coronary versus noncoronary versus right coronary cusp	.563
Base versus rest of cusp	.031
Interaction	.705
Tukey test, base versus rest of cusp	
Left coronary	.056
Noncoronary	.028
Right coronary	.025

Tukey tests were carried out for significant factors to determine which cusps were responsible for the significance.

### Cusp Thickness Analysis

The intensity values and their corresponding thicknesses were used to calculate a calibration curve relating the x-ray intensity in the radiograph to actual tissue thickness. A resulting thickness map can be seen in Figure 1, *B*. Mean thickness values were obtained for the base and rest of the cusp regions on both the vessel analysis samples and the calibration samples.

### Statistical Analysis

To evaluate intraobserver variability in the vessel counting exercise, an intraclass reliability coefficient was determined. Preferred vessel orientation within the cusps and any vessel density differences between the three cusps of the valve were analyzed with a 2-way repeated-measures analysis of variance (ANOVA) run with cusp type (left coronary, noncoronary, and right coronary) and direction (circumferential and radial). Another 2-way repeated-measures ANOVA was used to determine any differences in total vessel density among the three cusps of the valve and between the two areas

of the valve (base and rest of the cusp). A third repeated-measures ANOVA was used to determine whether there was any difference in the distribution of vessels between cusps or cusp regions. A paired *t* test was used to see whether the thickness correction factor from fixation was significantly different between the two regions of the cusp. To detect cusp differences in thickness and region (base and the rest of the cusp), a 2-way repeated-measures ANOVA was used after the thickness values were corrected for fixation effects. A Tukey test was used for pairwise multiple comparisons after any repeated-measures ANOVA that showed significance. All statistical tests were carried out using Sigma Stat (SPSS Inc, Chicago, Ill), a commercially available software package, except for the intraclass correlation coefficient, which was run with the program available from the Chinese University of Hong Kong.

### Results

Multiple vessel counting on single samples revealed a high intrarater reliability, with a coefficient of 0.98. Measurement of vessel orientation revealed no significant difference between the number of vessels passing in the radial or circumferential directions either in the base region or in the rest of the cusp (Table 1A). Similar results were found for the left coronary, right coronary, and noncoronary cusps. Counts from the circumferential and radial directions were therefore combined, and no correction for directionality was made in the remainder of the analysis.

After the number of vessels per square millimeter was calculated for the two regions, a 2-way repeated-measures ANOVA found a significant difference between the vessel density within the region identified as the base and the region identified as the rest of the cusp. This trend held true for all three cusps in the valve, although it was only statistically significant for the noncoronary and right coronary cusps (Table 1B). Even though there appeared to be an increasing vessel density trend from left coronary to noncoronary to right coronary cusp, no statistical difference was found. Most vessel diameters were less than 20  $\mu\text{m}$ , with the occasional arteriole or venule having a diameter as great as 100  $\mu\text{m}$ .

The numbers of grids containing vessels in each region of the cusp were also determined. No significant difference was found between cusps, but there was a significant differ-

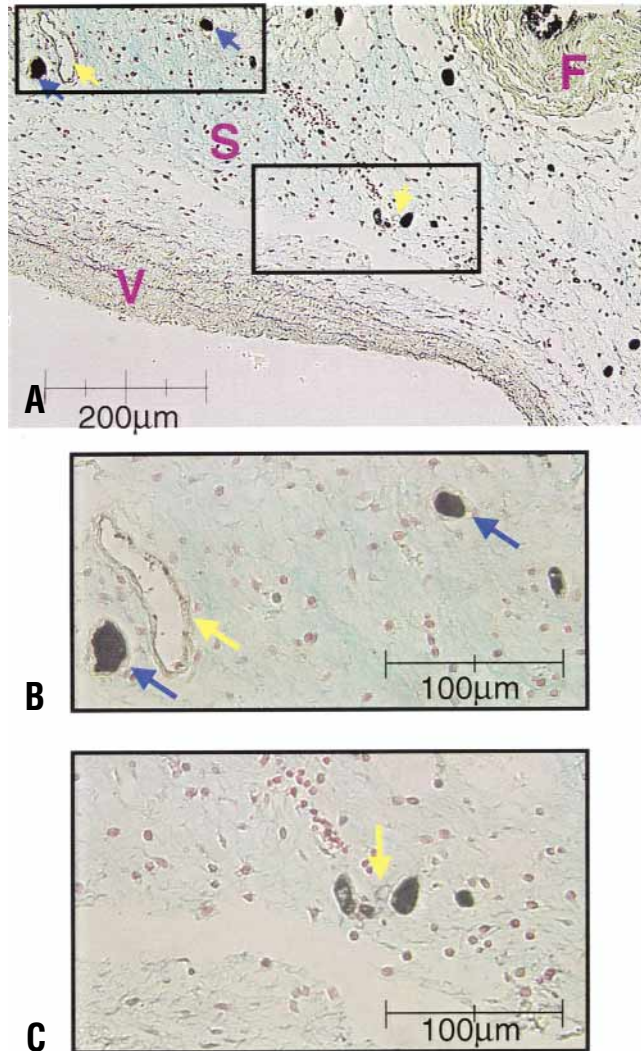


**Figure 4. A,** Porcine aortic valve cusp section at 100 $\times$  magnification stained with Movats pentachrome denoting 3 layers. **F,** Fibrosa; **S,** spongiosa; **V,** ventricularis. Note location of vasculature within spongiosa (vessel lumen appears black from Aquablack filling). **Blue arrows** point to examples of vessels filled with Aquablack; **yellow arrows** point to vessels where Aquablack filling did not occur. **B and C,** Two regions of interest outlined in A are shown at 200 $\times$  magnification to better visualize vessel lumen. **B,** Region at top in photo; **C,** lower region in photo.

ence when the base region, which had vessels in about 30% of its area, was compared with the rest of the cusp, where only 3% of the area was found to contain vessels in all three cusps (Table 2). An examination of the Movats pentachrome-stained slides revealed that these Aquablack-filled vessels were located within the spongiosal (middle) layer of the cusps (Figure 4).

A paired *t* test on the 14 cusps in the fresh versus fixed comparison results revealed that 10% formaldehyde treat-

### Thickness vs Vessels/mm<sup>2</sup> All Samples

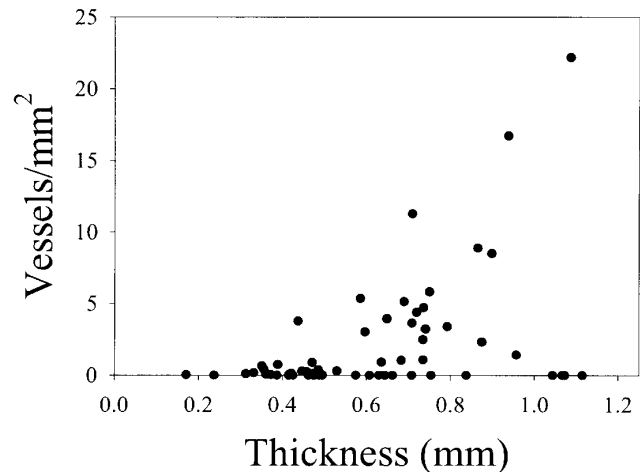


**Figure 5. Plot of cusp thickness versus vessel density showing both base and rest of cusp. Median vessel density of this plot is 5.16 vessels/mm<sup>3</sup>.**

ment had a significantly greater thickness increase on the rest of the cusp region than on the base region ( $P = .038$ ). Separate correction factors of 1/1.215 and 1/1.071, respectively, were therefore used to ascertain the true fresh thickness values of these two regions.

After determination of fresh thickness values for the base and the rest of the cusp regions, a 2-way repeated-measures ANOVA found a significant thickness difference between the two regions (Table 3). This test also revealed a significant difference between the base of the right coronary cusp and the base of the left coronary cusp, with the former being 20% thicker. Although the 15% difference between the base regions of the noncoronary cusp and the left coronary cusp did not quite reach statistical significance, there was a definite trend for the noncoronary cusp to be thicker. No significant differences were noted between the noncoronary and right coronary base thicknesses or between the thicknesses of the rest of the cusp regions in all three cusps making up the valve.

When thickness values were compared with the number of vessels, there was a trend for vessels to be present in tissue with a mean thickness greater than 0.5 mm (Figure 5). Of the 30 cusps examined, 9 cusps from 4 hearts were found to be avascular. This probably resulted from incomplete filling caused by the obstruction of a feeder vessel into these cusps. In fact, on histologic examination of one Movats-stained section from each cusp, vessels were visible in the base of 4 of the cusps found to be avascular according to the filling technique. However, no vessels were seen in the rest

**TABLE 2A. Percentage of cusp quadrants containing vessels**

Cusp	Base region	Rest of cusp
Left coronary	27.1% ± 21.1%	1.83% ± 1.77%
Noncoronary	33.9% ± 27.5%	3.13% ± 3.86%
Right coronary	27.8% ± 27.4%	3.07% ± 4.31%

of the cusp region, consistent with our vessel distribution findings determined with the Aquablack technique.

### Discussion

The presence of a blood supply within aortic valve tissue<sup>12</sup> implies that the tissue oxygen requirements exceed the amount deliverable by diffusion from the cusp surfaces alone. Although aortic valves function as mechanical devices, they contain a large cellular population, consisting predominantly of fibroblasts and myofibroblasts.<sup>20</sup> However, oxygen parameters such as consumption ( $VO_2$ ) or diffusion ( $DO_2$ ) of valve tissue have not been investigated. In fact, the only accounts we could find in the literature that determined these values at 37°C in vascular structures of the same species were those for the  $VO_2$  of the dog femoral artery, with a value of  $1.8 \times 10^{-4}$  mL  $O_2 \cdot mL$  tissue<sup>-1</sup> · s<sup>-1</sup>,<sup>21</sup> and the  $DO_2$  of the dog aorta adventitia, with a value of  $11.4 \times 10^{-6}$  cm<sup>2</sup> · s<sup>-1</sup>.<sup>22</sup> Because the valve is also a vascular structure, these values were used as a first approximation of oxygen transport within this tissue to see whether a reasonable tissue thickness that enabled oxygen delivery could be suggested. Solubility (k) of oxygen in plasma at 37°C is  $2.82 \times 10^{-5}$  mL  $O_2 \cdot mL$  tissue<sup>-1</sup> · mm Hg<sup>-1</sup>.<sup>23</sup> Water content of the valve is 90%,<sup>17</sup> and oxygen solubility of the valve cusp can therefore be estimated to be 90% of that for plasma, giving a value of  $2.54 \times 10^{-5}$  mL  $O_2 \cdot mL$  tissue<sup>-1</sup> · mm Hg<sup>-1</sup>. On the basis of these oxygen transport parameters and the assumption of a  $PaO_2$  of 100 mm Hg, and according the formula derived from the basic diffusion theory,<sup>24</sup> the estimated maximum distance that oxygen can be supplied from the cusp surface into the tissue ( $L_{max}$ ) is approximately 0.2 mm:

$$L_{max} = \sqrt{2 \cdot DO_2 \cdot k \cdot PO_2 / VO_2}$$

If valid, these data suggest that the aortic valve cusp must be less than 0.4 mm thick to avoid zero oxygen levels.

Our results show that the vascular supply of the aortic valve resides predominantly at the valve base, where we have shown tissue thickness to range from 0.692 to 0.860 mm. If we assume that the oxygen transport properties and the metabolic requirements of the valve approximate those of other vascular structures, our cusp thickness measure-

**TABLE 2B. Two-way repeated-measures ANOVA results comparing the percent of cusp quadrants containing vessels in the base region versus the rest of the cusp for all three cusps**

Factor	P value
Left coronary versus noncoronary versus right coronary cusp	.434
Base versus rest of cusp	.002
Interaction	.528
Tukey test, base vs rest of cusp	
Left coronary	.004
Noncoronary	<.001
Right coronary	.005

Tukey tests were carried out for significant factors to determine which cusps were responsible for the significance.

ments support the concept that an oxygen supply route in addition to that of diffusion from the cusp surfaces is necessary. Of course, actual oxygen consumption and oxygen diffusion measurements for aortic valve tissue will ultimately be required to confirm our conclusions.

From our thickness measurements it would also seem that the rest of the cusp area approaches the approximate diffusion distance limits and may require an additional oxygen supply route. However, studies on cusp collagen content have revealed that this area of the cusp contains large collagen bundles, with thicknesses on the average of 0.2 mm.<sup>17</sup> Interspersed between these bundles would be thinner, more optimal oxygen transport pathways that would aid in oxygen supply to these neighboring, thicker regions. In addition, it should be remembered that we measured cusp thickness in the relaxed state, corresponding to systole, and that tissue strain during valve closure will also affect thickness. The patterns of this strain distribution are complex, resulting in anisotropic thickness changes. Preliminary observations in our laboratory have revealed that thickness changes vary little in the base region during closure but that the area we consider to be the rest of the cusp can become as much as 40% thinner during diastole. This thickness change occurring in the rest of the cusp may also help to explain why a microcirculation is not necessary in this region. Finally, during closure the coapting area of the rest of the cusp region would no longer be able to obtain oxygen from both sides of the tissue, thereby having an effect on cusp oxygen parameters.

In determining  $L_{max}$ , we modeled the cusp as a homogeneous tissue. It is well established that the aortic valve cusp is a 3-layered structure,<sup>25</sup> and a more complex model that takes into account the heterogeneity of this tissue may pro-

**TABLE 3A. Mean cusp thickness in millimeters corrected for 10% formaldehyde fixation**

Cusp	Base region	Rest of cusp
Left coronary	0.692 ± 0.111	0.362 ± 0.107
Noncoronary	0.812 ± 0.197	0.475 ± 0.124
Right coronary	0.860 ± 0.171	0.482 ± 0.81

Correction factors for 10% formaldehyde fixation were Base fixed/1.071 = Base fresh and Rest of cusp fixed/1.215 = Rest of cusp fresh.

vide further insights into the oxygen supply properties. For example, it is more than likely that the outer, more collagenous layers will have lower oxygen diffusivity values than the middle spongiosa layer. This would probably decrease the oxygen available to the tissue from the surfaces of the cusp. Again, these issues highlight the importance of determining oxygen consumption and oxygen diffusion values for cusp tissue—and eventually even for the separate layers within the cusp—if we are to completely understand the oxygen parameters.

The microcirculation that we have shown to be present within the cusps can be described as a capillary bed with the occasional feeding arteriole and venule, according to vessel diameter.<sup>26</sup> It has been found to lie almost completely within the spongiosa layer, found in the middle of the cusp. The location of the vessels at the point of the lowest oxygen level supports the concept that a microcirculation is present within a cusp because of oxygen diffusion limitations from the cusp surfaces.

Also noted was a substantial variation in vessel density, with only 30% of the base region and only 3% of the rest of the cusp region being vascularized. Considering values obtained for mean thickness and vessels per square millimeter, the basal regions of the cusp showed similar average vessel densities of 4.92, 5.07, and 5.14 vessels/mm<sup>3</sup> for the left coronary, noncoronary, and right coronary cusps, respectively. In contrast, the average vessel density for the rest of the cusp region in all three cusps was approximately 0.659 vessels/mm<sup>3</sup>. Because only 30% of the base region and only 3% of the rest of the cusp were vascularized, however, averaging the number of vessels over the entire area created a significant vessel density dilution. In many cases the vessel density was as high as 15 vessels/mm<sup>3</sup> per grid area. Our observation of “blind ends” in the vasculature within some samples also indicated less than complete filling at times. This filling problem may explain the 9 cusps found to be avascular and suggests that our measurements represent a minimum cusp vessel density. Also in support of this, on histologic examination vessels not perfused with Aquablack were seen on several slides (Figure 4), including slides from those cusps found to be avascular. Such vessels

**TABLE 3B. Two-way repeated-measures ANOVA results (comparing mean cusp thickness in the base region versus rest of cusp for all three cusps)**

	P value
Thickness	
Left coronary versus noncoronary versus right coronary cusp	.007
Base versus rest of cusp	<.001
Interaction	.576
Tukey test	
Left coronary versus noncoronary versus right coronary cusp	
Left coronary versus right coronary	.008
Noncoronary versus right coronary	.767
Noncoronary versus left coronary	.034
Base versus rest of cusp	
Left coronary	<.001
Noncoronary	<.001
Right coronary	<.001

Tukey tests were carried out for significant factors to determine which cusps were responsible for the significance.

were still only noted in the basal region of the cusps. We therefore believe that our filling inconsistency resulted in random error, and even though the actual vessel densities reported may be low the overall distribution noted is more than likely real.

Although we have proposed that tissue thickness is a major factor in oxygen supply and demand, it is likely that additional factors play a role. The distribution of tissue stresses may be a significant factor, with ongoing tissue damage and repair mechanisms being an important determinant of vessel placement because the metabolic activity of these areas may exceed that of others. These issues will have to be explored as our understanding of the aortic valve's metabolic needs expands.

Our results indicate that the microcirculation within aortic valve cusps plays a role similar to that of the vasa vasorum of the aortic root. When designing tissue-engineered valve replacements to mimic normal living valve tissue, the addition of a microvasculature would add a high level of complexity and may be impractical. However, with a full understanding of cusp function and anatomy, a successful avascular replacement device could probably be created as long as overall thickness was maintained at approximately 0.4 mm. Evidence that an avascular valve implant in this thickness range can be successful is provided by the currently used Ross procedure, in which the pulmonary valve is transplanted to the aortic position. It has been demonstrated that this thinner valve structure can function well within the high-pressure environment of the left side of the

heart, despite the loss of blood supply.<sup>27</sup> This is presumably because of the pulmonary valve's ability to obtain adequate oxygen through diffusion from its surfaces when it is transplanted from its native  $P_{O_2}$  environment of 40 mm Hg to one of 100 mm Hg surrounding it in the aortic position. Yet valve cusps are intricate structures, with a delicate balance of components and subtle changes in design having the potential for enormous functional effects. Additional studies that define tissue characteristics, such as cellular density, as well as oxygen consumption and diffusion properties, are required to increase our understanding of the native valve and to assist in the development of a properly designed tissue-engineered valve replacement.

We thank Michael Thornton for assistance with the radiographic thickness measurements, Larry Stitt for statistical review, and Mount Bridges Abattoir for specimen supply.

#### References

- Sodian R, Hoerstrup SP, Sperling JS, Daebritz S, Martin DP, Moran AM, et al. Early in vivo experience with tissue-engineered trileaflet heart valves. *Circulation*. 2000;102(19 Suppl 3):III-22-9.
- Hoerstrup SP, Sodian R, Daebritz S, Wang J, Bacha EA, Martin DP, et al. Functional living trileaflet heart valves grown in vitro. *Circulation*. 2000;102(19 Suppl 3):III-44-9.
- Ferrans VJ, Spray TL, Billingham ME, Roberts WC. Structural changes in glutaraldehyde-treated porcine heterografts used as substitute cardiac valves: transmission and scanning electron microscopic observations in 12 patients. *Am J Cardiol*. 1978;41:1159-84.
- Hammermeister K, Sethi GK, Henderson WG, Grover FL, Oprian C, Rahimtoola SH. Outcomes 15 years after valve replacement with a mechanical versus a bioprosthetic valve: final report of the Veterans Affairs randomized trial. *J Am Coll Cardiol*. 2000;36:1152-8.
- O'Brien M, Stafford EG, Gardner MA, Pohlner PG, McGiffen DC, Kirklin JW. A comparison of aortic valve replacement with viable cryopreserved and fresh allograft valves, with a note on chromosomal studies. *J Thorac Cardiovasc Surg*. 1987;94:812-23.
- Angell WW, Oury JH, Lamberti JJ, Koziol J. Durability of the viable aortic allograft. *J Thorac Cardiovasc Surg*. 1989;98:48-56.
- Schoen FJ, Mitchell RN, Jonas RA. Pathological considerations in cryopreserved allograft heart valves. *J Heart Valve Dis*. 1995;4(Suppl 1):S72-5.
- Fischlein T, Schutz A, Haushofer M, Frey R, Uhlig A, Detter C, et al. Immunologic reaction and viability of cryopreserved homografts. *Ann Thorac Surg*. 1995;60 (2 Suppl):S122-6.
- Green M, Walsh MD, Dare A, Hogan PG, Zhao XM, Frazer IH, et al. Histologic and immunohistochemical responses after aortic valve allografts in the rat. *Ann Thorac Surg*. 1998;66(6 Suppl):S216-20.
- Zund G, Breuer CK, Shinoka T, Ma PX, Langer R, Mayer JE, et al. The in vitro construction of a tissue engineered bioprosthetic heart valve. *Eur J Cardiothorac Surg*. 1997;11:493-7.
- Ross D. The versatile homograft and autograft valve. *Ann Thorac Surg*. 1989;48(3 Suppl):S69-70.
- Weind KL, Ellis CG, Boughner DR. The aortic valve blood supply. *J Heart Valve Dis*. 2000;9:1-8.
- Hammon JW, O'Sullivan MJ, Oury J, Fosburg RG. Allograft cardiac valves: a view through the scanning electron microscope. *J Thorac Cardiovasc Surg*. 1974;68:352-60.
- Mayhew TM, Reith A. Introducing basic principles and methods of stereology and morphometry. In: Reith A, Mayhew TM, editors. *Stereology and morphology in electron microscopy: problems and solutions*. New York: Hemisphere Publishing; 1988. p. 1-12.
- White DR. Tissue substitutes in experimental radiation physics. *Med Phys*. 1978;5:467-9.
- White DR, Martin RJ, Darlison R. Epoxy resin based tissue substitutes. *Br J Radiol*. 1977;50:814-21.
- Scott MJ. The elastin and collagen microstructure of aortic heart valve cusps [dissertation]. London, Ontario, Canada: Univ. of Western Ontario; 1997.
- Fahrig R, Moreau M, Holdsworth DW. Three-dimensional computed tomographic reconstruction using a C-arm mounted XR2: correction of image intensifier distortion. *Med Phys*. 1997;24:1097-106.
- Weind KL, Ellis CG, Boughner DR. Porcine aortic valve cusp dimensional changes with aldehyde fixation [abstract]. *Can J Cardiol*. 2000; 16(Suppl):F-110.
- Messier RH, Bass BL, Aly HM, Jones JL, Domkowski PW, Wallace RB, et al. Dual structural and functional phenotypes of the porcine aortic valve interstitial population: characteristics of the leaflet myofibroblast. *J Surg Res*. 1994;57:1-21.
- Crawford DW, Cole MA, Back LH. Evidence for the blood oxygen boundary layer  $p_{O_2}$  gradient (change in  $p_{O_2}$ ) as a significant determinant of intimal (Pw) and lowest medial  $p_{O_2}$  (Pdn) in the vivo dog femoral artery. *Adv Exp Med Biol*. 1983;159:197-209.
- Buerk DG, Goldstick TK. Spatial variation of aortic wall oxygen diffusion coefficient from transient polarographic measurements. *Ann Biomed Eng*. 1992;20:629-46.
- Christoforides C, Laasberg LH, Hedley-Whyte J. Effect of temperature on solubility of  $O_2$  in human plasma. *J Appl Physiol*. 1969;26:56-60.
- Popel AS. Theory of oxygen transport to tissue. *Crit Rev Biomed Eng*. 1989;17:257-321.
- Gross L, Kugel MA. Topographic anatomy and histology of the valves in the human heart. *Am J Pathol*. 1931;7:445-73.
- Secomb TW. Mechanics of blood flow in the microcirculation. *Symp Soc Exp Biol*. 1995;49:305-21.
- Ross D, Jackson M, Davies J. The pulmonary autograft—a permanent aortic valve. *Eur J Cardiothorac Surg*. 1992;6:113-6.